Received XX Month 20XX; | Revised XX Month 20XX; | Accepted XX Month 20XX

DOI: xxx/xxxx

ARTICLE TYPE

# An Algorithm for Random Generation of Admissible Horizontal Alignments for Optimum Layout Design

Miguel E. Vázquez-Méndez*[1,2] | Gerardo Casal[1] | Alberte Castro[3] | Duarte Santamarina[1]

[1]Departamento de Matemática Aplicada, Universidade de Santiago de Compostela, Lugo, Spain

[2]Instituto de Matemáticas, Universidade de Santiago de Compostela, A Coruña, Spain

[3]Área de Enxeñaría e Infraestrutura dos Transportes. Departamento de Enxeñaría Agroforestal, Universidade de Santiago de Compostela, Lugo, Spain

***Correspondence**

Miguel E. Vázquez-Méndez, Universidade de Santiago de Compostela. Escola Politécnica Superior de Enxeñaría, Benigno Ledo, 27002 Lugo (Spain). Email: miguelernesto.vazquez@usc.es

**Abstract**

This work deals with the design of horizontal alignments for its application in intelligent civil systems. Two consecutive task are performed: the random generation of admissible horizontal alignments (alignments verifying some geometric constraints set in advance), and the optimal design of layouts joining two given points. A rigorous mathematical analysis of the first task leads to a novel algorithm for random generation of alignments, which is used to develop the global optimization method proposed for the second task. The usefulness of this approach is shown on some practical applications. First, two problems with applications in robotics, pipe layout design, and forest road design are solved in realistic situations. Next, the random generation of admissible horizontal alignments in mountainous terrain is addressed. Finally, the model is extended to 3D alignments and a real case study is presented, designing a bypass on the N-640 Spanish national road, surrounding the urban area of Monterroso.

**KEYWORDS:**

Horizontal alignment, global optimization, random multi-start, motion planning, Mixed Integer Non-Linear Programming (MINLP)

## 1 | INTRODUCTION

A horizontal alignment (HA) is a 2D polygonal chain, endowed with a series of horizontal curves smoothing the direction changes taking place between two consecutive tangent sections. The line segments of the polygonal chain are named main tangents, and the horizontal curves consist of a circular curve joined to two transition curves (see Figure 1 ). The design of a HA is a basic problem, both in robotics (Ravankar, Ravankar, Kobayashi, Hoshino, & Peng, 2018), and in the construction of any linear infrastructure (De Smith, 2006). It is the first stage (and probably the most important) in the process of road or railway design (Lee, Tsou, & Liu, 2009; Li, Pu, Schonfeld, Zhang, & Zheng, 2016).

In the pre-computer era, the design of alignments joining two given points was handmade, based on the experience and intuition of the engineer. The improvement of computers with high computational capabilities has inspired the application of mathematical techniques in this task (Bosurgi & D'Andrea, 2012; Shafahi & Bagherian, 2013; Vázquez-Méndez & Casal, 2016; Vázquez-Méndez, Casal, & Ferreiro, 2020) and, in particular, the number of papers related to the optimal design of alignments have shot up in the last decade (Kang & Schonfeld, 2020; Li et al., 2019; Mondal, Lucet, & Hare, 2015; Pu et al., 2019; Pushak, Hare, & Lucet, 2016; T. Song et al., 2020 in press; Z. Song, Yang, Schonfeld, Liu, & Li, in press; Sushma & Maji, 2020). Regardless of the design variables used, the objective desired, or the restrictions imposed, these optimization problems are usually non-convex (with several local minima), and they must be solved with a global optimization method. In many cases, the problem is tackled with an *ad-hoc* technique, based on genetic algorithms or other

[0]**Abbreviations:** HA Horizontal Alignment; AHA Admissible Horizontal Alignment; VA Vertical Alignment; NLP Non-Linear Programming; MINLP, Mixed Integer Non-Linear Programming; IP, Intersection Points; HIP, Horizontal Intersection Points

heuristic methods (Li et al., 2017; Maji & Jha, 2009). Classical optimization methods need initial alignments to start the algorithm (Li et al., 2016; Mondal et al., 2015). Usually, these alignments are obtained manually, using the characteristic of each case study, which greatly hinders the automation of the process (Sushma & Maji, 2020). Random generation of HA verifying pre-set geometric constraints, named *admissible horizontal alignments* (AHA), is a very useful tool to automate the use of many of the classic optimization methods. Being able to directly apply these classical methods is very valuable *per se* (intrinsically), but it is also helpful for comparing and verifying the *ad-hoc* algorithms proposed in the literature.

Fully automatic methods for generating and optimizing admissible alignments have been already proposed in the last two decades (see, for instance, Sushma & Maji (2020) and therein references). Most of those methods do not take into account transition curves and, moreover, the automatic procedure to obtain an AHA is not completely random. It is usually joined to the optimization process, linked to penalization techniques (Jong & Schonfeld, 2003), or through modifications or redesigns of a first unfeasible path (Li et al., 2016; Pu et al., 2019). In this paper a novel method to generate a fully random AHA is proposed. This algorithm is completely independent of the case study and of any optimization process, and therefore the generation of AHA is almost instantaneous. The first part of the paper is focused on this task, from a mathematical and computational point of view. In Section 2 simple conditions are established to guarantee the admissibility of a HA. As a result (Section 3), an algorithm is proposed, that randomly generates an AHA between any two given points. The usefulness of this random generation is illustrated in the second part of the work (Section 4), where the design of a new HA is stated within the framework of the Mixed Integer Non-Linear Programming (MINLP). The proposed method to solve this problem is based on the previous algorithm, which generates the multi-start prior to the optimization process. This model is tested by two examples with important applicability in intelligent civil systems, and the results are discussed and compared with those reported in the literature, for both academic problems. The model is also shown as a useful tool for generating AHA in mountainous terrain, and finally (Section 5), the geometric design of highways and railways is addressed. Both, the MINLP model and the numerical algorithm proposed to solve it, are extended to work with 3D alignments, and used in a real case study, to obtain a bypass on the N-640 Spanish national road, surrounding the urban area of Monterroso. The paper ends (Section 6) with some brief and interesting conclusions.

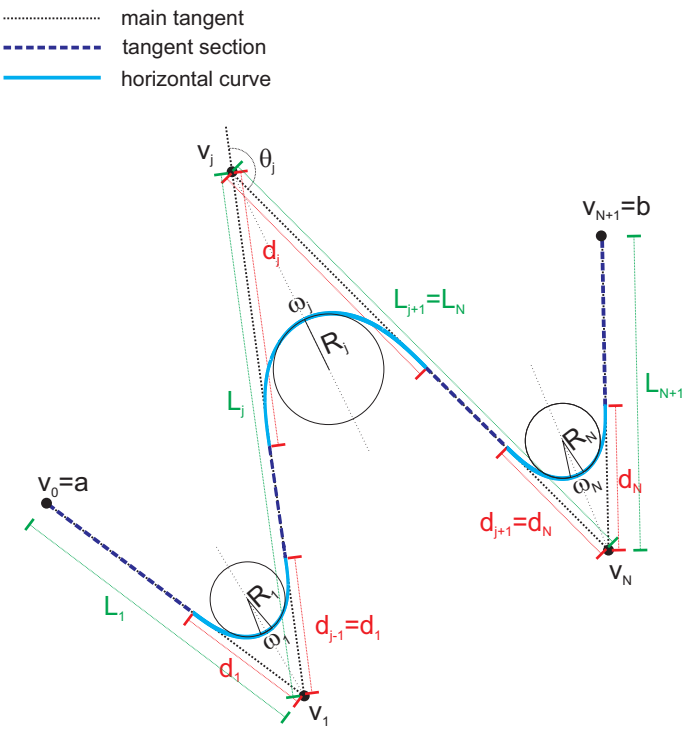


**FIGURE 1** Diagram of a HA: main components and notation.

## 2 | ADMISSIBLE HORIZONTAL ALIGNMENTS (AHA)

This section analyzes the admissibility of a HA connecting two given points $a, b \in \mathbb{R}^2$. Let $N$ be the number of horizontal curves, $v_0 = a$ and $v_{N+1} = b$ the starting and end points (terminals), and in what follows, $j$ and $k$ sub-index vary from 1 to N, and from 1 to $N+1$, respectively. Additionally, in this work the following hypotheses are assumed: (i) transition curves must be clothoid arcs, (ii) horizontal curves must be symmetrical with respect to the bisector of the angle formed by the corresponding main tangents, and (iii) each horizontal curve (the $j$-th curve) must be held inside the triangle of vertices $v_{j-1}$, $v_j$ and $v_{j+1}$ (see Fig. 1 ). Particularly, loop, horseshoe, and egg and double-egg curves are not considered.

Under previous hypothesis, a HA is uniquely defined by the vertices $v_j \in \mathbb{R}^2$ (also called IPs or HIPs for horizontal intersection points) determining the $N+1$ main tangents, and the radii $R_j \geq 0$ and angles $\omega_j \geq 0$ of the circular curves (see Figure 1 ).

Technical constraints must be verified in order to have an AHA (AASHTO, 2018). In this paper the following are considered:

$$R_j \geq R^{min}, \tag{1}$$
$$0 \leq \omega_j < \theta_j \leq \theta^{max}, \tag{2}$$
$$R_j(\theta_j - \omega_j) \geq L_C^{min}, \tag{3}$$
$$L_k - (d_k + d_{k-1}) \geq L_T^{min}, \tag{4}$$

where $R^{min} > 0$ is the minimum allowable radius of the layout design, $\theta_j$ is the deflection angle at the $j$-th curve (see Figure 1 ), $\theta^{max} \in (0, \pi)$ is the maximum allowable deflection angle, $L_C^{min} > 0$ and $L_T^{min} > 0$ are, respectively, the minimum length of each clothoid arc and each tangent section, $L_k$ is the length of the $k$-th main tangent (distance between $v_{k-1}$ and $v_k$) and, finally, $d_0 = d_{N+1} = 0$ and $d_j$ is the necessary distance to embed the $j$-th curve between the two corresponding main tangents (see Figure 1 ). Constraint (2) bounds and links the angle of the circular curve with the corresponding deflection angle, while (1), (3) and (4), respectively, establish lower bounds for radii and lengths of clothoids and tangent sections of the HA.

If the values of radius $R_j \geq R^{min}$ and angle $\omega_j \in [0, \theta^{max})$ are set, the necessary distance to embed the $j$-th curve between the corresponding main tangents depends exclusively on the deflection angle $\theta_j$, fulfilling (Casal, Santamarina, & Vázquez-Méndez, 2017)

$$d_j(\theta_j) = x_j^E(\theta_j) + y_j^E(\theta_j) \tan\left(\frac{\theta_j - \omega_j}{2}\right) + \left(R_j + \frac{y_j^E(\theta_j)}{\cos\left(\frac{\theta_j - \omega_j}{2}\right)}\right) \frac{\sin\left(\frac{\omega_j}{2}\right)}{\sin\left(\frac{\pi - \theta_j}{2}\right)}, \tag{5}$$

where

$$x_j^E(\theta_j) = \int_0^{R_j(\theta_j - \omega_j)} \cos\left(\frac{\tau^2}{2R_j^2(\theta_j - \omega_j)}\right) d\tau,$$
$$y_j^E(\theta_j) = \int_0^{R_j(\theta_j - \omega_j)} \sin\left(\frac{\tau^2}{2R_j^2(\theta_j - \omega_j)}\right) d\tau.$$

Thus, after the technical constraints are set ($R^{min}$, $\theta^{max}$, $L_C^{min}$ and $L_T^{min}$), and the radii ($R_j$) and the angles ($\omega_j$) are fixed, bounds can be found for $\theta_j$ and $L_k$ in order to guarantee that the corresponding HA is admissible. As will be shown in the next section, these bounds will be very useful for the random generation of alignments. In particular, the following result holds:

**Theorem 1.** Let $R_j \geq R^{min}$ and $\omega_j \geq 0$ be radii and angles verifying that

$$\frac{L_C^{min}}{R_j} + \omega_j \leq \theta^{max}, \tag{6}$$

and denote

$$\theta_j^{min} = \frac{L_C^{min}}{R_j} + \omega_j, \tag{7}$$
$$L_k^{min} = L_T^{min} + \left(d_k(\theta^{max}) + d_{k-1}(\theta^{max})\right). \tag{8}$$

If the following statement holds

$$\theta_j \in [\theta_j^{min}, \theta^{max}], \tag{9}$$
$$L_k \geq L_k^{min}, \tag{10}$$

then the HA is admissible.

*Proof.* The hypothesis (6) ensure that $[\theta_j^{min}, \theta^{max}] \neq \emptyset$, and that for any $\theta_j \in [\theta_j^{min}, \theta^{max}]$ constraints (1)-(3) hold. Furthermore, using Leibnitz's rule

$$\frac{dx_j^E}{d\theta_j} = R_j \cos\left(\frac{\theta_j - \omega_j}{2}\right) + \int_0^{R_j(\theta_j - \omega_j)} \frac{\tau^2}{2R_j^2(\theta_j - \omega_j)^2} \sin\left(\frac{\tau^2}{2R_j^2(\theta_j - \omega_j)}\right) d\tau,$$

which is clearly positive in $[\theta_j^{min}, \theta^{max}]$. Likewise,

$$\begin{aligned}\frac{dy_j^E}{d\theta_j} &= R_j \sin\left(\frac{\theta_j - \omega_j}{2}\right) - \int_0^{R_j(\theta_j - \omega_j)} \frac{\tau^2}{2R_j^2(\theta_j - \omega_j)^2} \cos\left(\frac{\tau^2}{2R_j^2(\theta_j - \omega_j)}\right) d\tau \\ &\geq R_j \sin\left(\frac{\theta_j - \omega_j}{2}\right) - \int_0^{R_j(\theta_j - \omega_j)} \frac{\tau^2}{2R_j^2(\theta_j - \omega_j)^2} d\tau \\ &= R_j \left(\sin\left(\frac{\theta_j - \omega_j}{2}\right) - \frac{\theta_j - \omega_j}{6}\right) \geq 0\end{aligned}$$

where the last inequality is a consequence of $f(x) = \sin x - x/3 \geq 0$, $x \in [0, \pi/2]$. Thus, functions $x_j^E$, $y_j^E$ are positive and increasing in $[\theta_j^{min}, \theta^{max}]$. Functions

$$f_j(\theta_j) = \tan\left(\frac{\theta_j - \omega_j}{2}\right), \quad g_j(\theta_j) = \frac{1}{\cos\left(\frac{\theta_j - \omega_j}{2}\right)},$$
$$h_j(\theta_j) = \frac{\sin\left(\frac{\omega_j}{2}\right)}{\sin\left(\frac{\pi - \theta_j}{2}\right)},$$

are also positive and increasing in $[\theta_j^{min}, \theta^{max}]$, and therefore $d_j$ is too. As a result

$$\begin{aligned}L_k - \left(d_k + d_{k-1}\right) &\geq L_k - \left(d_k(\theta^{max}) + d_{k-1}(\theta^{max})\right) \\ &= L_k - L_k^{min} + L_T^{min} \geq L_T^{min},\end{aligned}$$

and the HA is admissible. □

It should be highlighted that (10) is only a sufficient (not necessary) condition to guarantee that a HA is admissible.

The lower bound given in (8) is valid for any deflection angle verifying (9), but for each pair $(\theta_{j-1}, \theta_j)$, the best (necessary) lower bound for the length of the corresponding main tangent is $L_T^{min} + d_j(\theta_j) + d_{j-1}(\theta_{j-1})$. Consequently, there might be HA not verifying (10) which are AHA, that is, some AHA can be overlooked. To give an idea of the thresholds required in Theorem 1, Tables 1 and 2 show, respectively, the values of $d_j(\theta^{max})$ and $\theta_j^{min}$ for different radii $R_j$ and angles $\omega_j$, taking $\theta^{max} = \pi/2$ rad and $L_C^{min} = 95$ m as technical constraints.

## 3 | RANDOM GENERATION OF AN AHA

The aim of this section is to develop an algorithm allowing the random generation of an AHA joining two terminals $a, b \in \mathbb{R}^2$.

### 3.1 | Modification of a given AHA

Firstly, a modification of a main tangent of an AHA is studied, to incorporate between its two vertices, a new one (a new horizontal curve), in a way that the resulting HA remains admissible. For that purpose we focus on the situation shown in Figure 2 : a main tangent of length $L$ is considered bounded by vertices $v_{\text{down}}$ and $v_{\text{up}}$, the aim is to find angles ($\alpha \geq 0$ and $\beta \geq 0$) that the new main tangents (the first one starting from $v_{\text{down}}$ and the later reaching $v_{\text{up}}$) form with the old one. As a first step, the requirements over $\alpha$ and $\beta$ are given in order to keep the admissibility of the new HA.

**Deflection angle on existing vertices.** If the vertices are not the terminals, connected with $v_{\text{down}} \neq a$ and $v_{\text{up}} \neq b$ there are assumed curves with radii ($R_{\text{down}}$, $R_{\text{up}}$) and angles ($\omega_{\text{down}}$, $\omega_{\text{up}}$), which define –see Eq. (7)– lower bounds ($\theta_{\text{down}}^{min}$, $\theta_{\text{up}}^{min}$) held for the deflection angles. As shown in Figure 2 , these thresholds, in addition with $\theta^{max}$ and the current deflection angles ($\theta_{\text{down}}$, $\theta_{\text{up}}$), determine the admissible directions for any new main tangent starting from $v_{\text{down}}$ (bounds $\alpha_-^{max}$, $\alpha_+^{max}$), and for any arriving to $v_{\text{up}}$ (bounds $\beta_-^{max}$, $\beta_+^{max}$). Specifically, the following constraints must be verify

$$0 \leq \alpha \leq \alpha^{max}, \tag{11}$$

$$0 \leq \beta \leq \beta^{max}, \tag{12}$$

where $\alpha^{max} = \alpha_+^{max}$, $\beta^{max} = \beta_+^{max}$ if the new vertex is looked for *above* the main tangent to modify, and $\alpha^{max} = \alpha_-^{max}$, $\beta^{max} = \beta_-^{max}$ if it is looked for *below*. The detailed computation of $\alpha_-^{max}$, $\alpha_+^{max}$, $\beta_-^{max}$ and $\beta_+^{max}$ is shown in the flowchart shown in Fig. 3 .

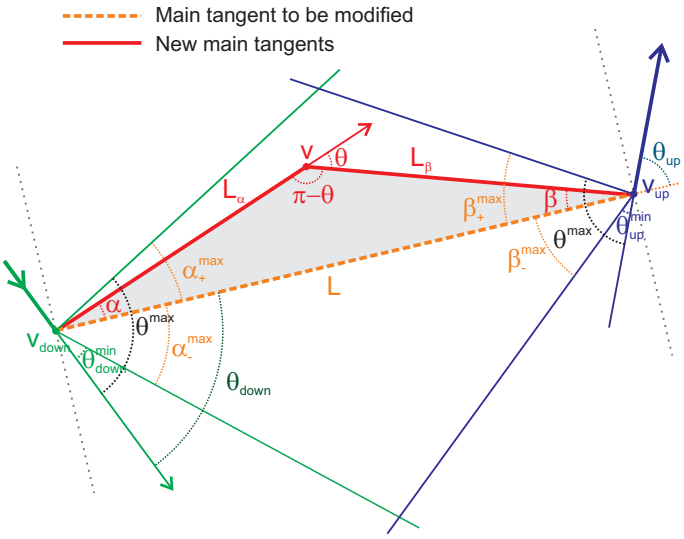


**FIGURE 2** Diagram for the modification of a main tangent of an AHA. Basic elements and notation.

**Deflection angle in the new vertex.** Associated with the new vertex a curve of radius $R \geq R^{min}$ and angle $\omega \geq 0$ is created. These elements $(R, \omega)$ define –Eq. (7)– a minimum bound $\theta^{min}$ for the deflection angle. The deflection angle in the new vertex is $\theta = \alpha + \beta$ and, therefore, the following inequalities must be fulfilled

$$\theta^{min} \leq \alpha + \beta \leq \theta^{max} \tag{13}$$

**Minimum lengths of the new main tangents.** Taking into account the radius and angle of the new curve, and those associated to the curves of vertices $v_{\text{down}}$ and $v_{\text{up}}$, the minimum lengths of the main tangents ($L_\alpha^{min}$, $L_\beta^{min}$) can be computed –Eq. (8)–. Naming as $L_\alpha$ and $L_\beta$ the lengths of these main tangents, and using the Law of Sines, the following relation can be obtained (see Figure 2 )

$$\frac{L_\alpha}{\sin\beta} = \frac{L_\beta}{\sin\alpha} = \frac{L}{\sin(\alpha+\beta)}.$$

From these equalities, constraints $L_\alpha \geq L_\alpha^{min}$ and $L_\beta \geq L_\beta^{min}$ are rewritten as

$$\frac{\sin\beta}{\sin(\alpha+\beta)} \geq \frac{L_\alpha^{min}}{L}, \tag{14}$$

$$\frac{\sin\alpha}{\sin(\alpha+\beta)} \geq \frac{L_\beta^{min}}{L}. \tag{15}$$

At this point, the main questions are: can angles $\alpha \geq 0$ and $\beta \geq 0$ exist verifying (11)-(15)? And, if they exist, how can be randomly generated? The first question finds its response in the following theorem. Its proof is fully constructive and leads directly to Algorithm 1 which answers the second question.

**TABLE 1** Values of $d_j(\pi/2)$ (in meters) computed by Eq. (5), for different radii and angles

| | $\omega_j$ =0 rad | $\omega_j$ =0.1 rad | $\omega_j$ =0.2 rad | $\omega_j$ =0.3 rad | $\omega_j$ =0.4 rad | $\omega_j$ =0.5 rad |
|---|---|---|---|---|---|---|
| $R_j$ = 100 m | 187.0 | 181.1 | 175.2 | 169.3 | 163.5 | 157.8 |
| $R_j$ = 150 m | 280.5 | 271.6 | 262.8 | 254.0 | 245.3 | 236.6 |
| $R_j$ = 200 m | 374.0 | 362.1 | 350.3 | 338.6 | 327.0 | 315.5 |
| $R_j$ = 300 m | 561.0 | 543.2 | 525.5 | 508.0 | 490.5 | 473.3 |
| $R_j$ = 400 m | 748.0 | 724.3 | 700.7 | 677.3 | 654.1 | 631.0 |
| $R_j$ = 500 m | 935.0 | 905.3 | 875.9 | 846.6 | 817.6 | 788.8 |

**TABLE 2** Values of $\theta_j^{min}$ (in radians) computed by Eq. (7) for different radii and angles, assuming that the minimum length of clothoid arcs is 95 m.

| | $\omega_j$ =0 rad | $\omega_j$ =0.1 rad | $\omega_j$ =0.2 rad | $\omega_j$ =0.3 rad | $\omega_j$ =0.4 rad | $\omega_j$ =0.5 rad |
|---|---|---|---|---|---|---|
| $R_j$ = 100 m | 0.950 | 1.050 | 1.150 | 1.250 | 1.350 | 1.450 |
| $R_j$ = 150 m | 0.633 | 0.733 | 0.833 | 0.933 | 1.033 | 1.133 |
| $R_j$ = 200 m | 0.475 | 0.575 | 0.675 | 0.775 | 0.875 | 0.975 |
| $R_j$ = 300 m | 0.316 | 0.416 | 0.516 | 0.616 | 0.716 | 0.816 |
| $R_j$ = 400 m | 0.237 | 0.337 | 0.437 | 0.537 | 0.637 | 0.737 |
| $R_j$ = 500 m | 0.190 | 0.290 | 0.390 | 0.490 | 0.590 | 0.690 |

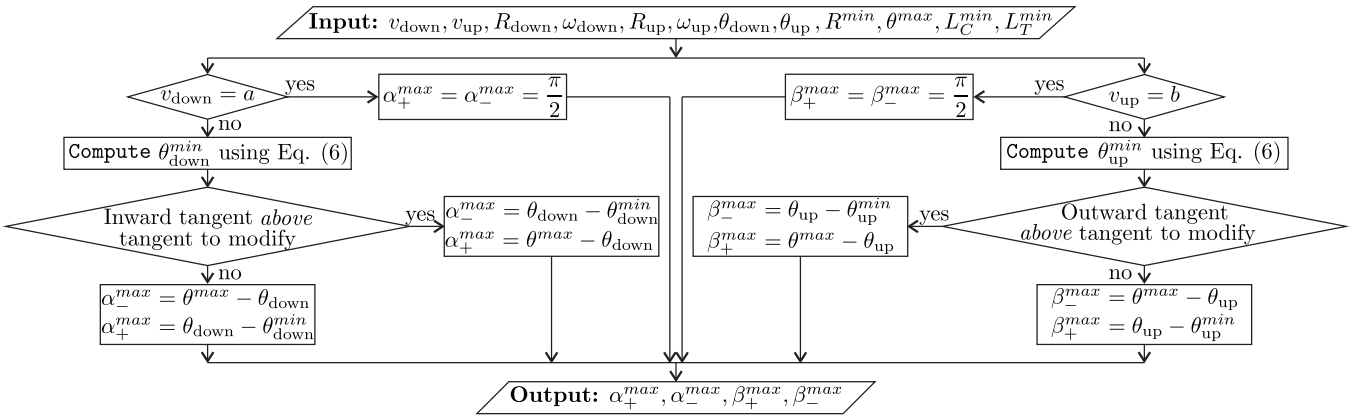


**FIGURE 3** Flowchart giving the computation of admissible directions for any new main tangent starting from $v_{\text{down}}$, and for any arriving to $v_{\text{up}}$.

**Theorem 2.** Let us suppose

$$L_\alpha^{min} \le L, \qquad L_\beta^{min} \le L, \tag{16}$$

and denote

$$\phi_\alpha^{min} = \arcsin\left(\frac{L_\beta^{min}}{L}\right), \quad \phi_\beta^{min} = \arcsin\left(\frac{L_\alpha^{min}}{L}\right). \tag{17}$$

If the following inequalities are verified

$$\phi_\alpha^{min} \le \alpha^{max}, \quad \phi_\beta^{min} \le \beta^{max}, \tag{18}$$

$$\theta^{min} \le \alpha^{max} + \beta^{max}, \tag{19}$$

$$\phi_\alpha^{min} + \phi_\beta^{min} \le \theta^{max}, \tag{20}$$

then, there exist angles $\alpha$ and $\beta$ simultaneously verifying conditions (11)-(15) and, consequently, the new HA remains admissible.

*Proof.* Let us define

$$\underline{\alpha} = \max\{\phi_\alpha^{min}, \theta^{min} - \beta^{max}\}, \tag{21}$$
$$\overline{\alpha} = \min\{\theta^{max} - \phi_\beta^{min}, \alpha^{max}\}. \tag{22}$$

Taking into account that $\theta^{max} \geq \theta^{min}$, hypothesis (18)-(20) ensure that $\underline{\alpha} \leq \overline{\alpha}$, that is, $[\underline{\alpha}, \overline{\alpha}] \neq \emptyset$. Taking $\alpha \in [\underline{\alpha}, \overline{\alpha}]$ randomly, let define

$$\underline{\beta_\alpha} = \max\{\phi_\beta^{min}, \theta^{min} - \alpha\}, \tag{23}$$
$$\overline{\beta_\alpha} = \min\{\theta^{max} - \alpha, \beta^{max}\}. \tag{24}$$

As $\alpha \in [\underline{\alpha}, \overline{\alpha}]$, from the definition of $\overline{\alpha}$ results

$$\theta^{max} - \alpha \geq \theta^{max} - \overline{\alpha} \geq \theta^{max} - (\theta^{max} - \phi_\beta^{min}) = \phi_\beta^{min},$$

and, as $\theta^{max} \geq \theta^{min}$, therefore $\theta^{max} - \alpha \geq \underline{\beta_\alpha}$. In the same way, hypothesis (18) and the definition of $\underline{\alpha}$ leads to $\beta^{max} \geq \underline{\beta_\alpha}$, and hence $\overline{\beta_\alpha} \geq \beta_\alpha$. Let $\beta \in [\beta_\alpha, \overline{\beta_\alpha}]$, the proof of the theorem will be completed by checking that angles $\alpha$, $\beta$ fulfill (11)-(15):

$$0 \leq \underline{\alpha} \leq \alpha \leq \overline{\alpha} \leq \alpha^{max},$$

$$\alpha \geq \underline{\alpha} \geq \phi_\alpha^{min} \Rightarrow \sin\alpha \geq \frac{L_\beta^{min}}{L}$$
$$\Rightarrow \frac{\sin\alpha}{\sin(\alpha+\beta)} \geq \sin\alpha \geq \frac{L_\beta^{min}}{L},$$

and, taking into account that $\beta \in [\underline{\beta_\alpha}, \overline{\beta_\alpha}]$, inequalities (12) and (15) are extrapolated in the same way. Finally,

$$\underline{\beta_\alpha} \leq \beta \leq \overline{\beta_\alpha} \Rightarrow \theta^{min} - \alpha \leq \beta \leq \theta^{max} - \alpha$$
$$\Rightarrow \theta^{min} \leq \alpha + \beta \leq \theta^{max}.$$

□

*Remark 1.* The choice taking place at line 2 of Algorithm 1 can be random ($R \in [R^{min}, R^{max}]$, $\omega \in [0, \omega^{max}]$, for $R^{max}$ and $\omega^{max}$ given values), but can also be supervised. If the generation of the AHA is built to *start* an optimization algorithm, intuition suggests (although it is not proven) that the main variables are the vertices (IPs) of the alignment. In that case, $R$ and $\omega$ may be chosen in such a way that the corresponding values of $\theta^{min}$ and $L^{min}$ help in the random generation of the main tangents.

## 3.2 | Generation of a new AHA

To generate an AHA, with at most $N^C$ curves, joining two given points $a$, $b \in \mathbb{R}^2$, the suggested method is based on *mathematical induction*: it is known that with $N^C = 0$ curves there is only one AHA (the tangent joining terminals $a$ and $b$), then assuming to have an AHA with $n$ curves, Algorithm 1 shows how to modify it (randomly) to get a new one, with $n+1$ curves. Thus, from the tangent joining $a$ and $b$ an AHA with one curve is created, from that, another with two curves, and so on until $N^C$ curves are accomplished or the procedure stops facing the impossibility to generate an AHA with an additional curve anymore.

**Algorithm 1** Modification to include between two consecutive IPs a new one

**Input:** Data of main tangent to be modified ($v_{\text{down}}$, $v_{\text{up}}$, $\theta_{\text{down}}$, $\theta_{\text{up}}$, $R_{\text{down}}$, $\omega_{\text{down}}$, $R_{\text{up}}$, $\omega_{\text{up}}$), and technical constraints ($R^{min}$, $\theta^{max}$, $L_C^{min}$, $L_T^{min}$)

**Output:** Vertex ($v$), radius ($R$) and angle ($\omega$) determining the new AHA between $v_{\text{down}}$ and $v_{\text{up}}$

1: `Compute` $\alpha_-^{max}$, $\alpha_+^{max}$, $\beta_-^{max}$ and $\beta_+^{max}$ as described in Fig. 3
2: `Choose` $R \geq R^{min}$ and $\omega \geq 0$ verifying (6)
3: `Compute` $\theta^{min}$, $L_\alpha^{min}$, $L_\beta^{min}$ by using Eq. (7) and Eq. (8)
4: **if** Eq. (16) is not verified **then**
5: `Print` "Main tangent cannot be modified to include the new curve"
6: `Stop`
7: **else**
8: `Compute` $\phi_\alpha^{min}$ and $\phi_\beta^{min}$, by using Eq. (17)
9: `Randomly choose` $sign \in \{+, -\}$
10: `Take` $\alpha^{max} = \alpha_{sign}^{max}$, $\beta^{max} = \beta_{sign}^{max}$
11: **if** Eq. (18)-(20) are not verified **then**
12: `Take` $\alpha^{max} = \alpha_{\text{opposite } sign}^{max}$, $\beta^{max} = \beta_{\text{opposite } sign}^{max}$
13: **end if**
14: **if** Eq. (18)-(20) are verified **then**
15: `Compute` $\underline{\alpha}$ and $\overline{\alpha}$, by using Eq. (21) and Eq. (22)
16: `Randomly choose` $\alpha \in [\underline{\alpha}, \overline{\alpha}]$
17: `Compute` $\underline{\beta_\alpha}$ and $\overline{\beta_\alpha}$, by using Eq. (23) and Eq. (24)
18: `Randomly choose` $\beta \in [\underline{\beta_\alpha}, \overline{\beta_\alpha}]$
19: `Compute` the new vertex $v$ by intersecting main tangents determined by $v_{\text{down}}$ and $\alpha$, and $v_{\text{up}}$ and $\beta$
20: **else**
21: `Print` "Main tangent cannot be modified to include the new curve"
22: **end if**
23: **end if**

To create an AHA with $n+1$ curves starting from one with $n$, a main tangent is chosen randomly, and this one is modified to generate a new curve with the method described in Algorithm 1. If it is not possible to generate the vertex, another main tangent is chosen (randomly among those not previously discarded), stopping the process if it is impossible to modify any of them.

The complete process to generate a random AHA joining two given points $a$, $b \in \mathbb{R}^2$, with at most $N^C$ curves, is described in Algorithm 2.

*Remark 2.* Line 8 of Algorithm 2 takes into account that if a main tangent is modified, the previous and the posterior

**Algorithm 2** Random generation of AHA joining two terminals $a, b \in \mathbb{R}^2$, with at most $N^C$ curves.

**Input:** Terminals ($a$, $b \in \mathbb{R}^2$), maximum number of curves ($N^C$), and technical constraints ($R^{min}$, $\theta^{max}$, $L_C^{min}$, $L_T^{min}$)
**Output:** Number of curves ($N$), Vertices ($v_j$), radii ($R_j$) and angles ($\omega_j$) determining the AHA.

Initialization: $N = 0$, $v_0 = a$, $R_0 = 0$, $\omega_0 = 0$, $v_1 = b$, $R_1 = 0$, $\omega_1 = 0$, $\text{Tang}_{\text{ad}} = \{1\}$
**while** $N < N^C$ and $\text{Tang}_{\text{ad}} \neq \emptyset$ **do**
  `Randomly choose` $k \in \text{Tang}_{\text{ad}}$
  `Run` Algorithm 1 taking indexes down $= k - 1$ and up $= k$
  **if** print "Main tangent cannot be modified to include the new curve" **then**
    `Take` $\text{Tang}_{\text{ad}} = \text{Tang}_{\text{ad}} - \{k\}$
  **else**
    `Take` $\text{Tang}_{\text{ad}} = \text{Tang}_{\text{ad}} \cup (\{k-1, k+1\} \cap \{1, \dots, N+1\})$
    **for** $i \leftarrow N$ **to** $k$ **do**
      `Take` $v_{i+1} = v_i$, $R_{i+1} = R_i$, $\omega_{i+1} = \omega_i$
      **if** $i \in \text{Tang}_{\text{ad}}$ **then**
        `Take` $\text{Tang}_{\text{ad}} = \left(\text{Tang}_{\text{ad}} - \{i\}\right) \cup \{i+1\}$
      **end if**
    **end for**
    `Take` $v_k = v$, $R_k = R$, $\omega_k = \omega$, $\text{Tang}_{\text{ad}} = \text{Tang}_{\text{ad}} \cup \{k\}$
    `Take` $N = N + 1$
  **end if**
**end while**

become candidates for modification (even if they were discarded in an earlier step). This is due to the fact that, after a main tangent is modified, the values of $\beta_+^{max}$ and $\beta_-^{max}$ change for the previous main tangent, and the values of $\alpha_+^{max}$ and $\alpha_-^{max}$ for the later. Thus, even if the conditions (18)-(20) were not fulfilled before, it might be possible that they do it now.

## 4 | APPLICATIONS TO OPTIMAL LAYOUT DESIGN

As it was mentioned in Section 2, if $N$ denotes the number of curves, a HA is univocally determined by vector

$$\mathbf{x}^N = (x_1, y_1, R_1, \omega_1, \dots, x_N, y_N, R_N, \omega_N) \in \mathbb{R}^{4N},$$

where $x_j$ and $y_j$ are the coordinates of the vertices (IPs) of the main tangents, namely $v_j = (x_j, y_j)$. The optimal design of HA involves solving a certain optimization problem, where the design variable (decision variable) is vector $\mathbf{x}^N$. In the framework of Mixed Integer Non-Linear Programming (MINLP), the formulation of the problem is

$$\min_{\mathbf{x}^N \in \mathbb{R}^{4N}} \quad J(\mathbf{x}^N) \tag{25}$$
$$\text{subject to} \quad \text{constraints (1)-(4)}, \tag{26}$$
$$0 \leq N \leq N^{max}, \tag{27}$$

where:

- $J(\mathbf{x}^N)$ is the objective function and depends on the specific problem to study. Its definition is what is known as *model*, and it is built taking into account economic and ecological aspects, safety, etc. In the following sections, three examples with different applicability in intelligent civil systems are presented.
- $N^{max} \in \mathbb{N}$ is the maximum number of curves allowed on the layout.

Admitting that $N^{max}$ is not a large value, problem (25)-(27) can be solved by doing an exhaustive search on the integer variable $N$. Therefore, for each $N = 1 \dots, N^{max}$, the problem (25)-(26) is solved with that fixed value of $N$, and the best of the $N^{max}$ obtained solutions is taken as the final result. For each fixed $N$, depending on the model used, problem (25)-(26) can be framed, or not, into differentiable optimization. In any case, the constraints, and also the objective function, are usually non-convex, and it is necessary to use global optimization techniques to solve that problem. Random generation of AHA is a very useful tool to develop these global optimization strategies. If a genetic algorithm is being used, Algorithm 2 allows us, for example, to obtain the initial population. In contrast, if a multi-start of a non linear programming (NLP) method is used, Algorithm 2 is the perfect tool allowing us to generate that random multi-start.

Algorithm 2 provides an AHA fulfilling constraints (1)-(4), but the exact number of curves is not previously known. In this paper a probability is assigned to the number of curves $N^C \in \{1, \dots, N^{max}\}$ that, at most, will have each randomly generated AHA. For this purpose, a set of values $\{p_i \in [0,1],\ i = 1, \dots, N^{max}\}$ is fixed, verifying

$$\sum_{i=1}^{N^{max}} p_i = 1,$$

and the problem (25)-(27) is directly solved, combining an appropriate NLP method with a random multi-start given by Algorithm 2, in such a way that, for each start, the probability of $N^C = i$ is $p_i$ ($p(\{N^C = i\}) = p_i$). The number of multi-starts ($M_S$) should be adapted to each case study and, particularly, it should be an increasing function of $N^{max}$. The method proposed to solve problem (25)-(27) is detailed in Algorithm 3 which, as shown, is straightforward to parallelize.

Following below, three applications are presented: two models for optimum layout design and one method for generating

**Algorithm 3** Method use to solve problem (25)-(27).

**Input:** Terminals ($a$, $b \in \mathbb{R}^2$), technical constraints ($R^{min}$, $\theta^{max}$, $L_C^{min}$, $L_T^{min}$), maximum number of curves ($N^{max}$), number of multi-starts ($M_S$), percentage of multi-starts desired with at most $i$ curves ($p_i$, $i = 1, \dots, N^{max}$), and objective function $J$ to be minimized

**Output:** Optimal decision vector $\mathbf{x}^N$ given the AHA joining terminals $a$ and $b$.

1: **for** $m \leftarrow 1$ to $M_S$ **do**
2: `Choose` $N_m^C \in \{1, \dots, N^{max}\}$ with probabilities $p(\{N^C = i\}) = p_i$
3: `Compute` $(\mathbf{x}_{inic}^N)_m$ by running Algorithm 2 with $N^C = N_m^C$
4: `Compute` a local minimum of (25)-(26), starting from $(\mathbf{x}_{inic}^N)_m$
5: **end for**
6: `Take` $\mathbf{x}^N$ as the best local minimum obtained for problem (25)-(26).

AHA in the geometry design of railways in mountainous terrain. Three models are differentiable, and to solve problem (25)-(26) –line 4 of Algorithm 3– an interior point method described in Byrd, Hribar, & Nocedal (1999), Byrd, Gilbert, & Nocedal (2000) and Waltz, Morales, Nocedal, & Orban (2006) is used, which is already implemented in the MATLAB R2018a Optimization Toolbox. To illustrate the potential and advantages of this new combination, the results obtained in both models for optimum layout design will be compared with those already presented on academic examples in Casal et al. (2017), where an ad-hoc (manual) alignment was provided for the NLP method.

## 4.1 | Problem 1: Shortest layout avoiding obstacles

The first problem consists in finding the shortest layout joining two given points $a$, $b \in \mathbb{R}^2$, avoiding obstacles $A_1, \dots, A_{N_Z} \subset \mathbb{R}^2$. In this type of problems, of great application in civil engineering (Davey, Dunstall, & Halgamuge, 2017; Easa & Mehmood, 2008) and robotics (Ravankar et al., 2018), the objective function to minimize can be written as

$$J_1(\mathbf{x}^N) = L(\mathbf{x}^N) + \lambda \int_0^{L(\mathbf{x}^N)} \sum_{i=1}^{N_Z} \chi_{A_i}(\sigma_{\mathbf{x}^N}(s))\, ds,$$

where:

- $L(\mathbf{x}^N)$ and $\sigma_{\mathbf{x}^N}$ are, respectively, the length and the arc length parametrization of the HA given by $\mathbf{x}^N$. A detailed algorithm to compute this parametrization can be seen in Casal et al. (2017).
- $\lambda$ is a penalty parameter for crossing through the obstacles.
- $\chi_{A_i}$ is a smooth approximation of the characteristic function of region $A_i$.

As an example, it is considered an academic problem previously introduced in Casal et al. (2017). The aim is to join points $a = (0, 1)$ and $b = (5.2, 2.1)$, avoiding the circles centered in $c_1 = (1, 1)$, $c_2 = (2.3, 2.4)$ and $c_3 = (4.2, 1.3)$, and respective radii $r_1 = 0.6$, $r_2 = 0.9$ and $r_3 = 1$. The problem deals with looking for a layout with at most $N^{max} = 3$ curves, radii greater than $R^{min} = 0.05$, and lengths of clothoids and tangent sections greater than $L_C^{min} = 0.095$ and $L_T^{min} = 0.1$, respectively. The penalty parameter $\lambda$, and function $\chi_{A_i}$ for the circle $A_i$ are $\lambda = 10^4$, and

$$\chi_{A_i}(x, y) = (\max\{r_i^2 - ||(x, y) - c_i||^2, 0\})^2, \quad i = 1, 2, 3.$$

In Casal et al. (2017) optimum layouts with one, two and three curves were computed, starting from an *ad-hoc* AHA, close to the expected solution of the problem. On the contrary, this paper ignores all geometric information available, and looks for the solution by solving the MINLP (25)-(27) with Algorithm 3. To try to guarantee that the global optimum is found, a highly overdimensioned multi-start, with $M_S$ =10,000 elements (seeds), and probabilities $p(\{N^C = 1\}) = 0.2$, $p(\{N^C = 2\}) = 0.2$, and $p(\{N^C = 3\}) = 0.6$ is used. In addition, in the generation of each initial AHA (Algorithm 2) deflection angles lower than $\theta^{max} = \pi/2$ are required, and the radii and angles are chosen randomly in $[0.1, 0.5]$ and $[0, \pi/4]$, respectively (see Remark 1).

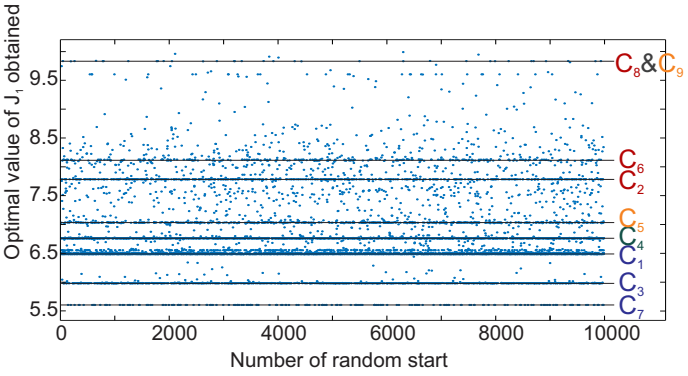


**FIGURE 4** Scatterplot with the values of objective function $J_1$, obtained by solving Problem 1 with a multi-start of 10,000 elements. The legend $C_j$ indicates that this value corresponds with the layout $C_j$ shown in the Figure 5 .

In 98% of the cases, the obtained solution manages to avoid the three obstacles. For these cases, the scatterplot of the values of the objective function $J_1$ is shown in Figure 4 . As shown

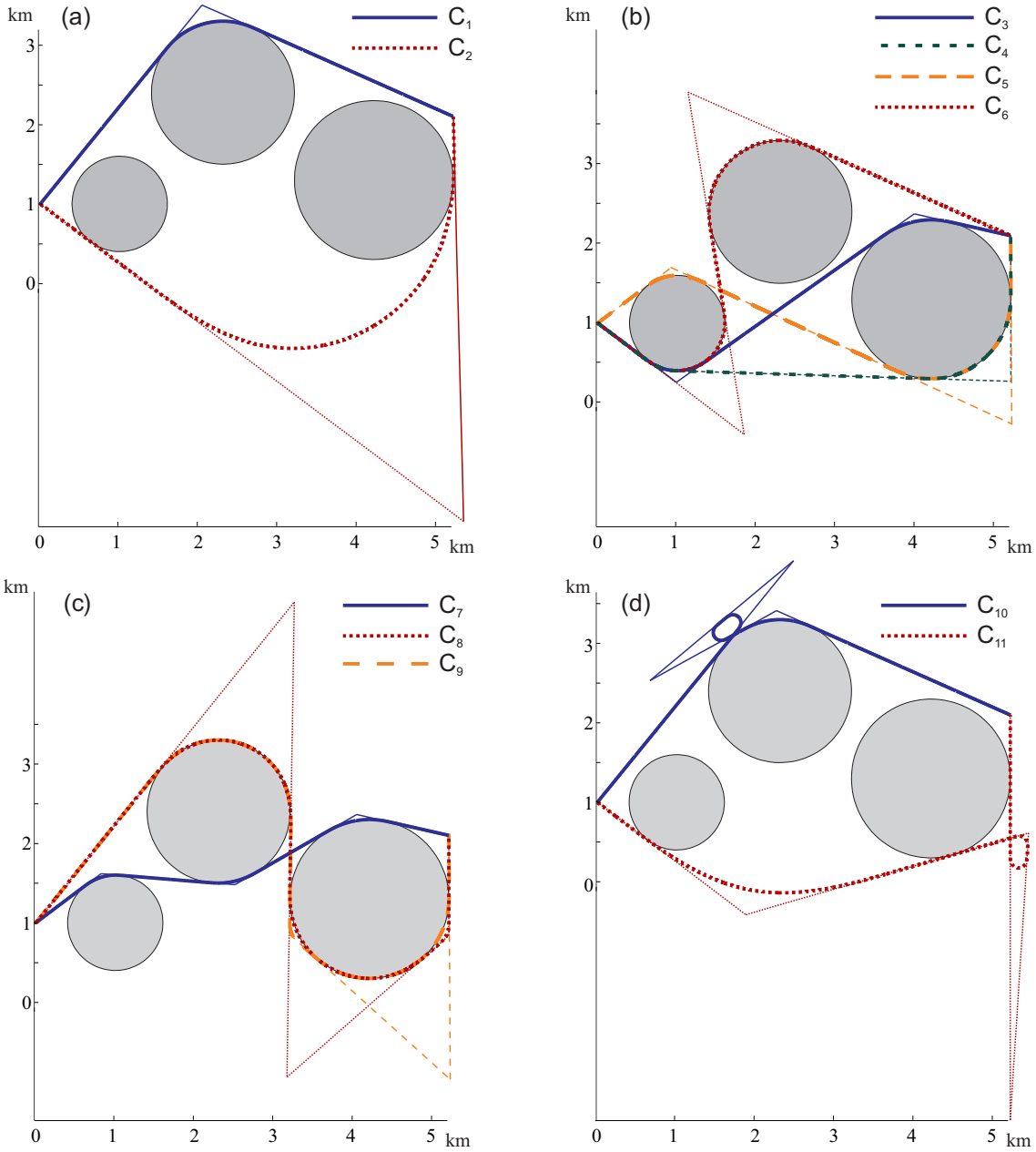


**FIGURE 5** Layouts corresponding to some of the local minima obtained by solving Problem 1 with Algorithm 3 (for each plot $C_j$, the corresponding value of $J_1$ can be seen in Figure 4 ). In particular, layout $C_7$ corresponds with the solution (global minimum) of Problem 1.

there, most (around 70%) of the obtained optima are gathered around 8 different values. After a close analysis of those solutions, it is observed that these values correspond with 9 local minima, whose corresponding graphs ($C_1$ to $C_9$) are shown in Figures 5 (a), 5 (b) and 5 (c). The other values correspond, either with false convergences, either with other less common local minima, such as those shown in Figure 5 (d).

Among the solutions shown in Figure 5 are the minima with one ($C_1$), two ($C_3$) and three curves ($C_7$) reported in Casal et al. (2017). In fact, the most frequently obtained layouts are the optima with one curve ($C_1$) and two ($C_3$), along with small variants of these with some additional curves. The global optimum ($C_7$) was reached 187 times, which gives an idea of the actual number of multi-starts required to successfully solve this problem. One experiment with $M_S$ =10,000 elements can be considered as 10,000 experiments with $M_S = 1$ element. Then, the probability of obtaining the global minimum with $M_S$ =1 can be assumed equal to 0.0187 (ratio of success over

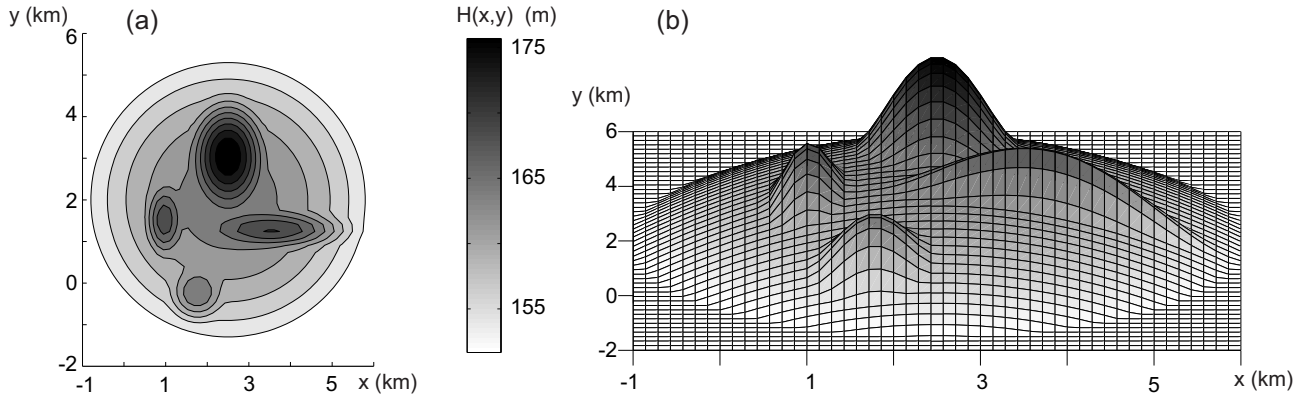


**FIGURE 6** Terrain for academic example solved in Problem 2: contour lines (a) and graphic representation (b) of function $H(x, y)$.

number of attempts) and, in the same way, the probability of finding it in a multi-start with $M_S$ =100 elements is 84.86%, while in one with $M_S = 200$ seeds rises up to 97.71%.

As discussed above, one of the advantages of Algorithm 3 is the ease of parallelization. A MATLAB (version 9.4 (R2018a)) code was developed to solve it. It was ran on a cluster with 8 PowerEdge R840 with Intel(R) Xeon(R) Gold 6126 processors, 12 cores per processor and 384GB of RAM. MATLAB proprietary parallelization was used with a number of 24 threads. The computation time to solve Problem 1 with $M_S$ =200 is, on average, 1042 seconds (particularly, the random generation of 200 AHA was around 0.1686 seconds).

Another advantage of Algorithm 3, compared to other methods of global optimization, is that not only provides the final solution of the problem, but also supplies other local minima that may be of great interest in Engineering. For example, in Civil Engineering it is common for designers to provide different alternatives (local minima), from which the final layout is chosen (Pushak et al., 2016). This election can be done based on additional criteria not previously considered in the optimization process. Thus, Figure 5 (a) shows two layouts with a single curve that provide a North ($C_1$) and a South ($C_2$) alternatives. $C_1$ is the best North layout but from the South, other option with two curves ($C_4$) is obtained that is substantially shorter (see Figure 5 (b)). Figure 5 (c) shows, in addition to the global optimum ($C_7$), two other solutions with three curves ($C_8$ and $C_9$), which are very similar to each other and with the same length. Finally, Figure 5 (d) shows, as an example, two other local minima found ($C_{10}$ and $C_{11}$). Both, with little practical interest, illustrate the robustness and versatility of the algorithm allowing the existence of backtracking and loops formed by two consecutive curves.

## 4.2 | Problem 2: Short length layout with low slope

The second problem that arises is the design of a short layout between two given points and passing through an area with low terrain slope. This problem has applications in robotics (Howard & Kelly, 2007), in pipe layout designs (De Smith, 2006), or forest roads with certain safety standards, trying to avoid major earthworks (Hay, 1998; Hearn & Hunt, 2011). If $H(x, y)$ is the function giving the ground elevation and $\sigma(s) = (\sigma_1(s), \sigma_2(s))$, $s \in [0, L]$, is a parametrization of the HA, the slope of each point on layout is given by

$$H'(s) = \frac{\partial H}{\partial x}(\sigma(s))\sigma_1'(s) + \frac{\partial H}{\partial y}(\sigma(s))\sigma_2'(s).$$

Therefore, the objective function to minimize

$$J_2(\mathbf{x}^N) = \epsilon L(\mathbf{x}^N) + (1-\epsilon)\int_0^{L(\mathbf{x}^N)} \left(\frac{\partial H}{\partial x}(\sigma_{\mathbf{x}^N}(s))\sigma_1'(s) + \frac{\partial H}{\partial y}(\sigma_{\mathbf{x}^N}(s))\sigma_2'(s)\right)^2 ds,$$

where $\epsilon \in [0, 1]$ is a weight parameter that quantifies the relevance of length of the HA versus slope of the layout (if the value of $\epsilon$ is close to zero, minimizing the slope is the main objective, and if it is close to one, the main objective lies to obtain a short HA).

In this second test, taking $J_2$ as objective function, the problem (25)-(27) is solved on academic example: the aim is to join points $a = (0.35, 1)$ and $b = (4, 2)$ with the shortest HA and the lowest possible slope, taking $\epsilon = 0.001$ as a weight parameter between both objectives, and considering that ground elevation is given by function $H(x, y)$ shown in Figure 6 .

As in Problem 1, to ensure that the global minimum is reached, an oversized multi-start with 10,000 elements is used. In addition, $N^{max} = 3$ is taken, and at each start $N^C$ is chosen with the same probability as in previous problem, guaranteeing

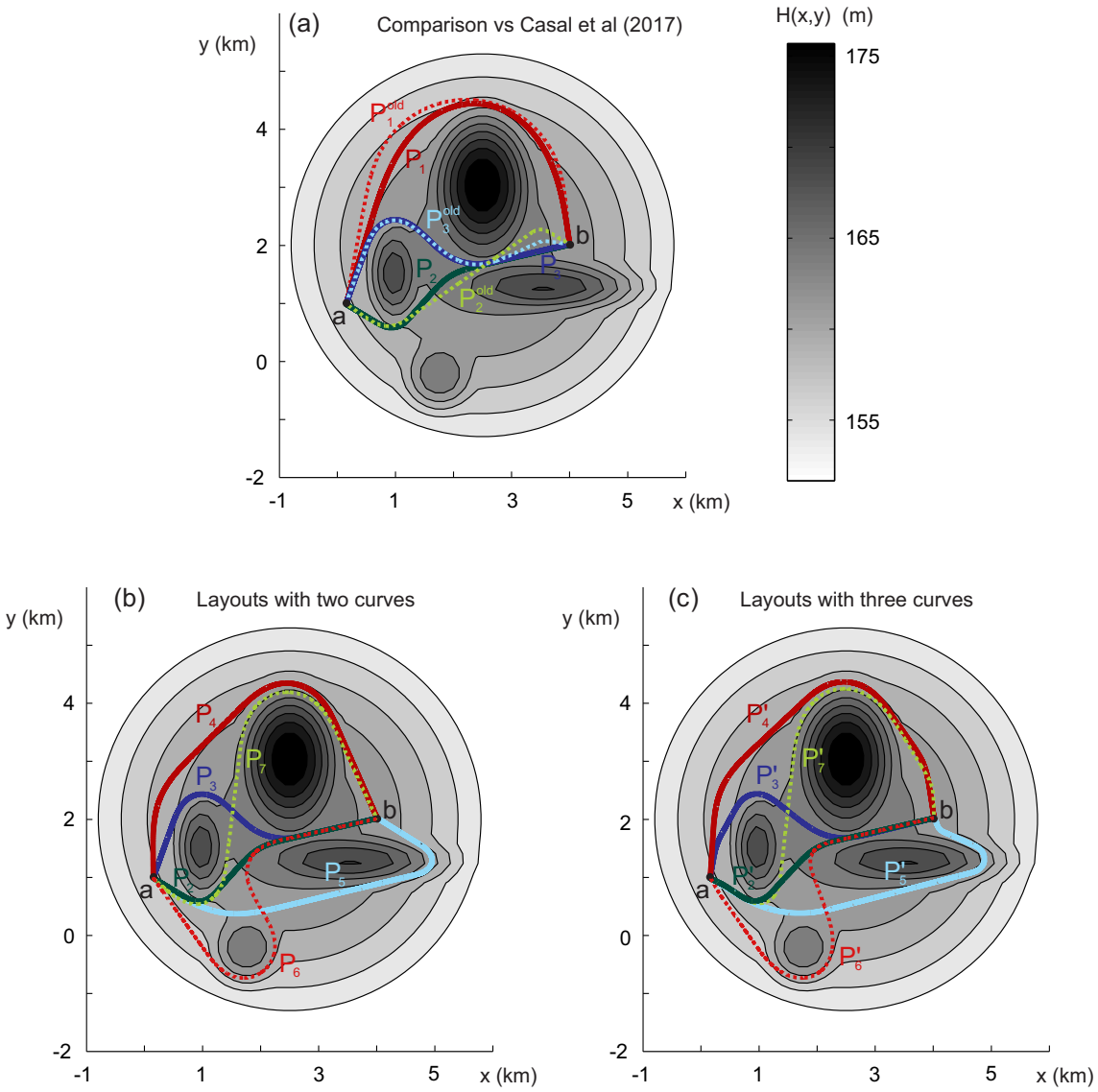


**FIGURE 7** Layouts corresponding to some local minimums of Problem 2: reported in Casal et al. (2017) ($P_n^{old}$) and obtained in this work with one and two curves ($P_n$), and with three curves ($P_n'$). Data and the objective function values $J_2$ are summarized in Table 3 .

deflection angles lower than $\theta^{max} = \pi/2$, and choosing radii and angles randomly within $[0.1, 0.5]$ and $[0, \pi/4]$, respectively.

The results obtained in this case confirm the existence of numerous local minima and, in practically all starts (99.84%), the interior points algorithm converge to one of them. In this case, the optimal layout obtained in Casal et al. (2017) with one, two and three curves are significantly improved. Figure 7 (a) shows the layouts reported in Casal et al. (2017) ($P_n^{old}$) and, to illustrate the improvement, they are compared with the corresponding solutions obtained in this new experiment ($P_n$). Data and values of function $J_2$ corresponding to each of these layouts can be seen in Table 3 .

It is important to highlight that the global minimum is reached practically with only two curves, something that was not observed in the previous work, were an *ad-hoc* (manual) AHA was chosen based on the geometry of the problem. Figure 7 (b) exhibits some of the layouts with two curves (local minima) obtained more frequently. Figure 7 (c) shows layouts with three curves (also in local minima) with objective functional values very similar to the previous ones (those with two curves). As shown, the layouts are very similar and, although the solutions with three curves have a slightly lower value of $J_2$ (see Table 3 ), the reduction is so small and the existence of an additional curve might not be justified.

**TABLE 3** Data and objective function values $J_2$ related to layouts ($P_n^{old}$, $P_n$ and $P_n'$) shown in Figure 7 .

| | $\mathbf{x}^N = (x_1, y_1, R_1, \omega_1, \dots, x_N, y_N, R_N, \omega_N)$ | $J_2(\mathbf{x}^N)$ |
|---|---|---|
| $P_1^{old}$ | (2.86, 14.99, 1.624, 2.190) | 0.0095 |
| $P_1$ | (2.87, 9.62, 1.110, 0.113) | 0.0093 |
| $P_2^{old}$ | (0.96, 0.52, 0.404, 0.160, 3.51, 2.29, 0.210, 0.431) | 0.0084 |
| $P_2$ | (1.07, 0.51, 0.313, 0.503, 1.99, 1.53, 0.947, 0.166) | 0.0073 |
| $P_2'$ | (0.51, 0.87, 0.925, 0.019, 1.06, 0.51, 0.309, 0.523, 2.02, 1.54, 0.923, 0.141) | 0.0073 |
| $P_3^{old}$ | (0.87, 2.72, 0.349, 0.094, 2.33, 1.51, 0.687, 0.046, 3.55, 2.06, 0.225, 0.138) | 0.0076 |
| $P_3$ | (0.89, 2.78, 0.359, 0.071, 2.16, 1.57, 0.956, 0.722) | 0.0076 |
| $P_3'$ | (0.35, 1.56, 0.953, 0.093, 0.93, 2.61, 0.340, 0.549, 2.25, 1.57, 0.958, 0.313) | 0.0075 |
| $P_4$ | (0.24, 2.37, 1.324, 0.154, 2.74, 4.85, 0.726, 0.776) | 0.0079 |
| $P_4'$ | (0.35, 2.56, 1.314, 0.211, 2.61, 4.69, 0.755, 0.980, 3.86, 2.89, 1.093, 0.108) | 0.0079 |
| $P_5$ | (1.35, 0.28, 1.513, 0.213, 5.26, 1.22, 0.177, 0.144) | 0.0088 |
| $P_5'$ | (1.48, 0.27, 1.840, 0.530, 5.29, 1.26, 0.213, 1.499, 4.08, 1.79, 0.146, 0.032) | 0.0083 |
| $P_6$ | (7.81, -9.63, 0.530, 1.726, 1.51, 1.45, 0.488, 0.640) | 0.0100 |
| $P_6'$ | (0.40, 0.73, 1.878, 0.002, 3.87, -4.19, 0.474, 0.324, 1.81, 1.48, 0.288, 0.550) | 0.0097 |
| $P_7$ | (1.33, 0.08, 0.420, 0.533, 2.06, 6.11, 0.705, 1.280) | 0.0106 |
| $P_7'$ | (1.35, 0.33, 0.313, 0.612, 1.96, 5.91, 0.696, 0.614, 3.99, 2.55, 0.560, 0.143) | 0.0105 |

Finally, it is worth to point out that the global minimum (layout $P_2$ or $P_2'$ in Figure 7 ) is obtained in 650 of the 10,000 seeds. The real number of multi-starts required to successfully solve this problem is lower than in the previous case (Problem 1). Assuming that the probability of obtaining the global minimum is 0.0650, the probability of finding it in a multi-start with 50 elements is 96.53%, while in one with 100 seeds rises up to 99.88%. Using the same cluster as in the previous example, the computational time to solve the Problem 2 with $M_S = 100$ has an average time 353 seconds (particularly, the random generation of 100 AHA was around 0.0769 seconds).

## 4.3 | Problem 3: Random generation of AHA in mountainous terrain

The geometric design of a highway or railway is determined by the HA, the vertical alignment (VA) and the cross sections defined along the infrastructure. The VA should verify bound constraints on the slope (gradient) of the main tangents. In mountainous terrain these constraints affect the HA and establish a minimum threshold for its length. Specifically, the following bound should be verified (Vázquez-Méndez, Casal, Santamarina, & Castro, 2021)

$$L(\mathbf{x}^N) \geq L_{min} = \frac{|H(a) - H(b)|}{m_{max}}, \tag{28}$$

where $H(a)$ and $H(b)$ are the terrain heights at terminals, and $m_{max}$ is the maximum slope threshold. In mountainous areas (if the difference of terrain heights at terminals is large with respect to the horizontal distance between them), the random AHA generated by Algorithm 2 may not verify (28). In this case, new "random" AHA verifying this constraint can be obtained by solving problem (25)-(26) with an appropriate objective function. For a given value $\Delta L > 0$, if

$$\begin{aligned} J_3(\mathbf{x}^N) = \quad & \left(\max\{0, L_{min} - L(\mathbf{x}^N)\}\right)^2 \\ & + \left(\max\{0, L(\mathbf{x}^N) - (L_{min} + \Delta L)\}\right)^2, \end{aligned}$$

then $J_3(\mathbf{x}^N) = 0$ if and only if $L(\mathbf{x}^N) \in [L_{min}, L_{min} + \Delta L]$. Therefore, if there exists an AHA verifying constraint (28), the solutions of problem (25)-(26), taking $J_3$ as objective function, reaches the value $J_3 = 0$. In this case, for each random AHA generated by Algorithm 2, problem (25)-(26) can be solved by a gradient-type algorithm, and the obtained solution is another "random" AHA verifying constraint (28).

As example, the case study presented in Li et al. (2016) is considered. A mountainous terrain, where the elevation difference between the start and end points is 336.90 m, while the horizontal distance is only 3672,95 m. The gradient between these terminals is 9.17%, greatly exceeding the maximum gradient 3% ($m_{max}$) provided by the authors. Figure 8 shows some AHA (9 layouts) obtained with the previous method, those were obtained after a computational time of 69.47 seconds. All of them verify (28), with a length between 11.2 km and 12.2 km, compiling also with other geometrical constraints (radii greater than 600 m, and tangents and horizontal circular curves greater than 60 m). As it is described in next section, these AHA could now be used for obtaining 3D admissible

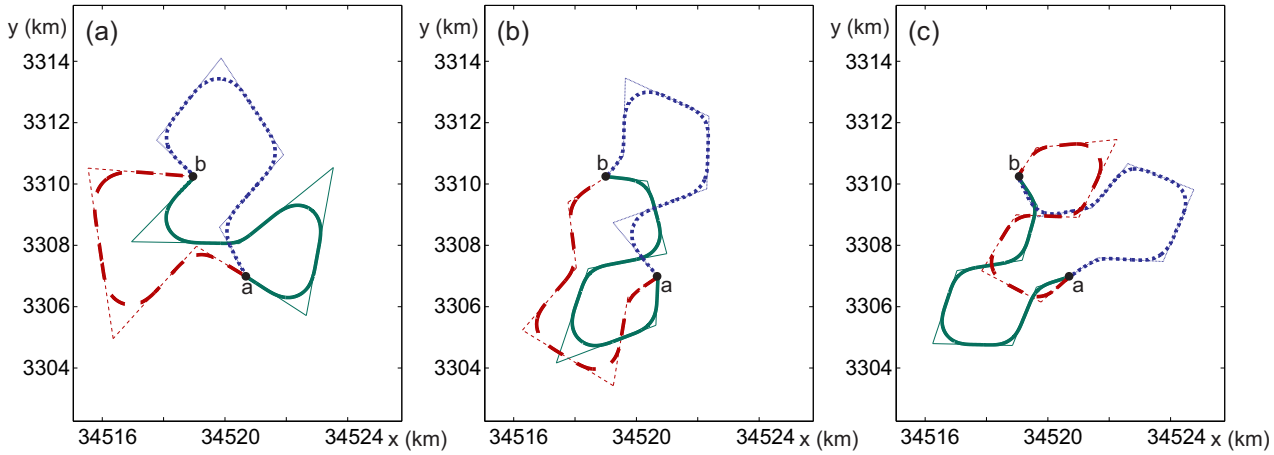


**FIGURE 8** Some random AHA with 3-4 curves (a), 5 curves (b) and 6 curves (c), corresponding to the case study presented in Li et al. (2016).

alignments which can be use, in turn, to start the railway design optimization process.

## 5 | CASE STUDY

For a geometric design of a highway or a railway line, the MINLP model (25)-(27) should be extended to include the optimal design of the VA. A VA is a 2D polygonal chain endowed with a series of curves smoothing the slope (gradient) changes taking place between two consecutive line segments (main tangents). These curves are assumed parabolic arcs, and the VA is completely determined by

$$\mathbf{y}^M = (s_1, m_1, K_{v1}, \dots, s_M, m_M, K_{vM}) \in \mathbb{R}^{3M},$$

where $M \in \mathbb{N}$ is the number of slope changes, $0 < s_1 < \dots < s_M < 1$ are the values that, once multiplied by the length of the HA, provide the coordinates of the VA vertices, $m_i \in \mathbb{R}$ is the slope of the $i$-th main tangent of the VA, and $K_{vi}$ defines the $i$-th parabolic arc (it is the ratio between the length of the parabolic section and the difference between two consecutive uniform slopes). Main constraints in VA design are

$$m_{min} \le |m_i| \le m_{max}, \tag{29}$$

$$K_{vi} \ge K_{vmin}, \tag{30}$$

$$L_i^{3D}(\mathbf{x}^N, \mathbf{y}^M) \ge L_{min}^{3D}, \tag{31}$$

where $L_i^{3D}(\mathbf{x}^N, \mathbf{y}^M)$ is the horizontal distance between two consecutive parabolic arcs, and $m_{min}$, $m_{max}$, $K_{vmin}$, $L_{min}^{3D} \ge 0$ are given thresholds.

The optimal geometric design of a 3D alignment (for example a highway or a railway line) can be formulated as the *extended* MINLP model

$$\min_{(\mathbf{x}^N, \mathbf{y}^M) \in \mathbb{R}^{4N+3M}} \quad J(\mathbf{x}^N, \mathbf{y}^M) \tag{32}$$

$$\text{subject to} \quad \text{constraints (1)-(4) and (29)-(31)}, \tag{33}$$

$$0 \le N \le N^{max}, \ 0 \le M \le M^{max}, \tag{34}$$

where $J(\mathbf{x}^N, \mathbf{y}^M)$ is the 3D model, and $M^{max}$ is the maximum number of slope changes allowed on the layout.

Algorithm 3 can be directly extended to solve this problem, and it is only necessary an algorithm to randomly compute $(\mathbf{x}_{inic}^N, \mathbf{y}_{inic}^M)$ verifying (1)-(4) and (29)-(31). In this paper, the following method is proposed:

**Step 1.** Compute $\mathbf{x}_{inic}^N$ verifying (1)-(4) and (28) by Algorithm 2, or as described in Section 4.3 if it is necessary.

**Step 2.** Chose $M \in \{1, \dots, M^{max}\}$ and compute $\mathbf{y}_{inic}^M = (s_1, m_1, K_{v1}, \dots, s_M, m_M, K_{vM})$ in the following way:

1. $s_i$ equi-spaced, that is, $s_i = i/(M+1)$.
2. $K_{vi} = K_{vmin}$.
3. Define $\bar{m} = (H(b) - H(a))/L(\mathbf{x}_{inic}^N)$ and $\Delta m = \frac{1}{3}\min\{|\bar{m}| - m_{min}, m_{max} - |\bar{m}|\}$, and take

   $\{m_1, \dots, m_M\} = \{\bar{m} + \Delta m, \bar{m} - \Delta m, \dots, \bar{m} + \Delta m\}$,

   if $M$ is odd, and

   $\{m_1, \dots, m_M\} = \{\bar{m}, \bar{m} + \Delta m, \bar{m} - \Delta m \dots, \bar{m} + \Delta m\}$,

   if $M$ is even.

To show the usefulness of our approach in a real-life problem, we focus our attention in designing a road bypass around Monterroso's town center, on a section around 3 km long of the two-lane Spanish national road N-640. All details of this real-world case study can be seen in (Vázquez-Méndez, Casal, Santamarina, & Castro, 2018), where a differentiable

**TABLE 4** Main data and total cost for North, South and Intermediate detours, shown in Figure 9 .

| | North detour | South detour | Intermediate detour |
|---|---|---|---|
| Length of the layout | 3,950 $m$ | 3,912 $m$ | 4,011 $m$ |
| Land acquisition area | 112,497 $m^2$ | 113,378 $m^2$ | 118,968 $m^2$ |
| Clearance area | 88,828 $m^2$ | 89,934 $m^2$ | 94,934 $m^2$ |
| Cut volume | 60,696 $m^3$ | 69,308 $m^3$ | 84,973 $m^3$ |
| Fill volume (re-used material) | 48,181 $m^3$ | 56,933 $m^3$ | 71,228 $m^3$ |
| Fill volume (acquired material) | 50 $m^3$ | 500 $m^3$ | 3,710 $m^3$ |
| Waste volume | 3,549 $m^3$ | 3,825 $m^3$ | 4,519 $m^3$ |
| **Total cost** | 3,769,736 € | 3,891,487 € | 4,063,922 € |

3D model has been proposed to optimize infrastructure costs in road design. That model can be included in the extended MINLP model (32)-(34), and in this work it has been solved by using Algorithm 3, extended as it was described above. Likewise in that previous work, $N^{max} = 4$ and $M^{max} = 3$ have been assumed. Then, $M_S = 200$ initial AHA have been generated with percentages of $N_i^C$ curves given by $p_1 = 0$, $p_2 = 0.2$, $p_3 = 0.2$ and $p_4 = 0.6$ (with a partial computation time of 0.1711 seconds). Each of those 200 initial AHA has been combined with VA with one, two and three slope changes (computed with the Step 2 of the previous procedure), resulting in a multi-start of 600 elements. After a total computation time of 4.02 $10^4$ seconds, three different optimal bypasses are obtained, whose correspond with the North, South and Intermediate detours shown in Figure 9 .

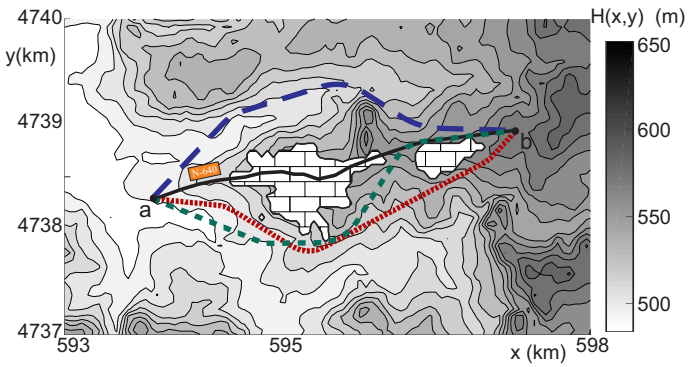


**FIGURE 9** North, South and Intermediate optimal detours (dashed lines) in the Spanish national road N-640 (solid line), obtained to avoid Monterroso's town center (bricked area).

Main data and total cost for North, South and Intermediate optimal detours are shown in Table 4 . The best solution from an economic point of view is the North detour. Comparing the results with those obtained in (Vázquez-Méndez et al., 2018), the cost of this new North (respectively South) detour is lowered by 3.6% (respectively 19.9%). Regardless of the improvement in economic terms, the main advantage of the new approach is that it is completely automatic (*ad-hoc* –manual– initial alignments are not necessary), and provides multiple optimal detours to the Civil Engineer, who can choose among them, taking into account other factors that may not have been considered in the optimization process.

## 6 | CONCLUSIONS

This paper studies the random generation of AHA and its application to the optimal layout design. Based on what was presented, it should be noted that:

- Sufficient conditions are given to generate an AHA, and also to be able to modify a main tangent of an AHA, including a new curve. In addition, an algorithm is proposed (Algorithm 1) describing how to develop this modification randomly.
- A method is provided (Algorithm 2) randomly generating an AHA between two given points. The method is completely independent of the case study (input data are only the terminals, the geometric constraints and the maximum number of curves) and of any optimization process, and therefore the generation of AHA is almost instantaneous.
- A general MINLP model is proposed for the optimal design of a HA, and a global optimization method is provided (Algorithm 3) to solve it. The suggested method evidences some relative benefits over existing approaches:
  - It works with all main elements of the HA, including transition curves.
  - No Geographical Information System (GIS data) is needed to provide an initial corridor.

  - It is easily parallelizable.
  - It not only gives the global optimum of the problem, but also provides other local minima that can be of great interests in engineering.

- The usefulness of this new method is tested by solving two problems, introduced in a previous work, that have considerable applications in intelligent civil systems. The results achieved show that:
  - The proposed method provides a fully automatic process to obtain the solution of the problem, without a previous geometric analysis.
  - The reported results in the literature, which use an *ad-hoc* (manual) AHA to start the optimization process, are significantly improved.
  - Computational times to solve both problems invite to use the method in more complex problems: problems with a larger dimension (where a greater number of curves are allowed), or where the evaluation of the objective function requires a longer calculation time.
  - Algorithm 3 can be used to compare and corroborate *ad-hoc* methods to be developed in future works. In particular, problems solved in this paper can serve as academic examples to test new methods.
- The MINLP model is also shown as an useful tool for generating AHA in the geometry design of railways in mountainous terrain.
- An *extended* MINLP model is proposed to work with 3D alignments and address the geometric design of highways and railways. The numerical method (Algorithm 3) is also extended to solve this problem, and this approach is tested in a real case study, previously introduced in the literature. The obtained results are very satisfactory, and encourage a detailed study about the random generation of 3D admissible alignments, which will be addressed in a future work.

In this paper most common geometric constraints on horizontal and vertical alignments are considered, but constraints on the alignment coordination, such as maximum rate between consecutive radii of horizontal curves, are not taken into account. These geometric criteria should be currently assessed by the designer and will be studied in future works. The efficiency in the topic of road alignment design of nature inspired optimization techniques, such as neural dynamic optimization (Adeli & Park, 1995), simulated annealing (Siddique & Adeli, 2016), and others will be also explored in a forthcoming research.

## ACKNOWLEDGMENTS

Third author thanks the support given by the Consellería de Cultura, Educación e Universidade (Xunta de Galicia) by Project ED431B 2020/25. The authors are also very grateful to the Editor and the seven anonymous reviewers for their very valuable suggestions.

## References

AASHTO. (2018). *A policy on geometric design of highways and streets, 7th edition*. Washington D.C.: American Association of State Highway and Transportation Officials.

Adeli, H., & Park, H. S. (1995). A neural dynamics model for structural optimization–Theory. *Computers & Structures*, *57*(3), 383–390.

Bosurgi, G., & D'Andrea, A. (2012). A polynomial parametric curve (ppc-curve) for the design of horizontal geometry of highways. *Computer-Aided Civil and Infrastructure Engineering*, *27*(4), 304–312.

Byrd, R. H., Gilbert, J. C., & Nocedal, J. (2000). A trust region method based on interior point techniques for nonlinear programming. *Mathematical Programming*, *89*, 149–185.

Byrd, R. H., Hribar, M. E., & Nocedal, J. (1999). An interior point algorithm for large-scale nonlinear programming. *SIAM Journal on Optimization*, *9*(4), 877–900.

Casal, G., Santamarina, D., & Vázquez-Méndez, M. E. (2017). Optimization of horizontal alignment geometry in road design and reconstruction. *Transportation Research Part C: Emerging Technologies*, *74*, 261–274.

Davey, N., Dunstall, S., & Halgamuge, S. (2017). Optimal road design through ecologically sensitive areas considering animal migration dynamics. *Transportation Research Part C: Emerging Technologies*, *77*, 478–494.

De Smith, M. J. (2006). Determination of gradient and curvature constrained optimal paths. *Computer-Aided Civil and Infrastructure Engineering*, *21*(1), 24–38.

Easa, S. M., & Mehmood, A. (2008). Optimizing design of highway horizontal alignments: New substantive safety approach. *Computer-Aided Civil and Infrastructure Engineering*, *23*(7), 560–573.

Hay, R. (1998). Forest road design. In FAO, ECE, ILO, *and* I*nternational* U*nion of* F*orestry* R*esearch* O*rganizations (*E*ds.),* P*roceedings of the seminar on environmentally sound forest roads and wood transport.* Roma: FAO.

Hearn, G. J., & Hunt, T. (2011). C1 route corridor and alignment selection. *Geological Society, London, Engineering Geology Special Publications*, *24*(1), 135–144.

Howard, T. M., & Kelly, A. (2007). Optimal rough terrain

trajectory generation for wheeled mobile robots. *The International Journal of Robotics Research*, *26*(2), 141–166.

Jong, J.-C., & Schonfeld, P. (2003). An evolutionary model for simultaneously optimizing three-dimensional highway alignments. *Transportation Research Part B: Methodological*, *37*(2), 107–128.

Kang, M.-W., & Schonfeld, P. (2020). *Artificial intelligence in highway location and alignment optimization*. World Scientific.

Lee, Y., Tsou, Y., & Liu, H. (2009). Optimization method for highway horizontal alignment design. *Journal of Transportation Engineering*, *135*(4), 217–224.

Li, W., Pu, H., Schonfeld, P., Song, Z., Zhang, H., Wang, L., … Peng, L. (2019). A method for automatically recreating the horizontal alignment geometry of existing railways. *Computer-Aided Civil and Infrastructure Engineering*, *34*(1), 71–94.

Li, W., Pu, H., Schonfeld, P., Yang, J., Zhang, H., Wang, L., & Xiong, J. (2017). Mountain railway alignment optimization with bidirectional distance transform and genetic algorithm. *Computer-Aided Civil and Infrastructure Engineering*, *32*(8), 691-709.

Li, W., Pu, H., Schonfeld, P., Zhang, H., & Zheng, X. (2016). Methodology for optimizing constrained 3-dimensional railway alignments in mountainous terrain. *Transportation Research Part C: Emerging Technologies*, *68*, 549–565.

Maji, A., & Jha, M. K. (2009). Multi-objective highway alignment optimization using a genetic algorithm. *Journal of Advanced Transportation*, *43*(4), 481–504.

Mondal, S., Lucet, Y., & Hare, W. (2015). Optimizing horizontal alignment of roads in a specified corridor. *Computers & Operations Research*, *64*, 130–138.

Pu, H., Song, T., Schonfeld, P., Li, W., Zhang, H., Wang, J., … Peng, X. (2019). A three-dimensional distance transform for optimizing constrained mountain railway alignments. *Computer-Aided Civil and Infrastructure Engineering*, *34*(11), 972–990.

Pushak, Y., Hare, W., & Lucet, Y. (2016). Multiple-path selection for new highway alignments using discrete algorithms. *European Journal of Operational Research*, *248*(2), 415–427.

Ravankar, A., Ravankar, A. A., Kobayashi, Y., Hoshino, Y., & Peng, C.-C. (2018). Path smoothing techniques in robot navigation: State-of-the-art, current and future challenges. *Sensors*, *18*(3170).

Shafahi, Y., & Bagherian, M. (2013). A customized particle swarm method to solve highway alignment optimization problem. *Computer-Aided Civil and Infrastructure Engineering*, *28*(1), 52-67.

Siddique, N., & Adeli, H. (2016). Simulated annealing, its variants and engineering applications. *International Journal on Artificial Intelligence Tools*, *25*(06), 1630001.

Song, T., Pu, H., Schonfeld, P., Zhang, H., Li, W., Hu, J., & Wang, J. (2020). Mountain railway alignment optimization considering geological impacts: A cost-hazard bi-objective model. *Computer-Aided Civil and Infrastructure Engineering*, *35*(12), 1365-1386.

Song, T., Pu, H., Schonfeld, P., Zhang, H., Li, W., Hu, J., … Wang, J. (in press). Bi-objective mountain railway alignment optimization incorporating seismic risk assessment. *Computer-Aided Civil and Infrastructure Engineering*.

Song, Z., Yang, F., Schonfeld, P., Liu, H., & Li, J. (in press). Integrating segmentation and parameter estimation for recreating vertical alignments. *Computer-Aided Civil and Infrastructure Engineering*.

Sushma, M. B., & Maji, A. (2020). A modified motion planning algorithm for horizontal highway alignment development. *Computer-Aided Civil and Infrastructure Engineering*, *35*(8), 818–831.

Vázquez-Méndez, M. E., & Casal, G. (2016). The clothoid computation: A simple and efficient numerical algorithm. *Journal of Surveying Engineering*, *142*(3), 04016005.

Vázquez-Méndez, M. E., Casal, G., & Ferreiro, J. B. (2020). Numerical computation of egg and double-egg curves with clothoids. *Journal of Surveying Engineering*, *146*(1), 04019021.

Vázquez-Méndez, M. E., Casal, G., Santamarina, D., & Castro, A. (2018). A 3D model for optimizing infrastructure costs in road design. *Computer-Aided Civil and Infrastructure Engineering*, *33*(5), 423–439.

Vázquez-Méndez, M. E., Casal, G., Santamarina, D., & Castro, A. (2021). Optimization of an urban railway bypass. A case study in A Coruña-Lugo line, Northwest of Spain. *Computers & Industrial Engineering*, *151*, 106935.

Waltz, R. A., Morales, J. L., Nocedal, J., & Orban, D. (2006). An interior algorithm for nonlinear optimization that combines line search and trust region steps. *Mathematical Programming*, *107*, 391–408.

**How to cite this article:** Vázquez-Méndez, M.; Casal, G.; Castro, A.; Santamarina, D.; An algorithm for random generation of admissible alignments for optimum layout design. *Computer-Aided Civil and Infrastructure Engineering*, 202X;XX:XX–XX.